Control Strategies for Front Stabilization in a Tubular Reactor Model

Vadim Panfilov and Moshe Sheintuch
Dept. of Chemical Engineering, Technion-Israel Institute of Technology, Haifa 32000, Israel

The stabilization of a front pattern in a homogeneous tubular reactor model was studied. Linear stability analysis combined with the Galerkin method is used for state-feedback control of the distributed parameter system. The capabilities of the global control and point-sensor control to stabilize the front solution were studied by manipulating various reactor parameters, including fluid flow and feed conditions. Point-sensor control in coolant flow (heat-loss coefficient) or coolant temperature are the most effective when the temperature sensor is located close to the front position. Global control based on a space-averaged sensor and other strategies failed. A qualitative analysis is suggested for selection of proper control of front stabilization.

Introduction

The theory of spatiotemporal pattern evolution is currently attracting considerable attention in various branches of the sciences and its applications to technological problems, like reactor design (such as Sheintuch and Shvartsman, 1996), are emerging. Problems of the pattern selection and control in systems with truly nonlinear dynamics are new academic topics, initiated by practical reasons like the control of a naturally chaotic state into a periodic or quasi-periodic orbit (Ott et al., 1990; see bibliography list with more than 500 entries in Chen, 1996).

Typically, patterned states may show large gradients in time (ignition, extinction) or in space (fronts, pulses). These appear in systems with wide separation of time and length scales that are common to many engineering systems. Several groups are currently developing basic principles of the control approaches to one-dimensional distributed systems for which a certain patterned state is advantageous or inevitable. The simplest patterned state is a stationary front that can emerge in a single variable diffusion–reaction system (that is, with no explicit convection). The front can easily be stabilized by (global) feedback control that is based on spatially averaged measurements. When a second variable is added, the front can be destabilized, resulting in a rich variety of patterns (Middya et al., 1994). Several ways for stabilizing such a front were suggested (Shvartsman and Kevrekidis, 1998; Panfilov and Sheintuch, 1999).

Convection of reactants is central to all fixed-bed reactors, and it affects the front velocity as it "pushes" the front downstream. In this work we study the stabilization of a stationary pattern in a simple homogeneous model of a tubular catalytic reactor for which several patterned states (stationary profiles) coexist. While many authors have addressed the control problem of a fixed-bed, they have not considered inhomogeneous patterned states like stationary fronts and typically they employed low, and unrealistic, *Pe* number values (such as Christofides and Daoutidus, 1996). Fronts that emerge in the model employed here are different from creeping fronts of fixed beds or from fronts in reaction–diffusion systems (see discussion below). The source of destabilization of the fronts in our model is a slow process of activation and deactivation. This work is an extension to series of recent articles in which we compared mechanisms of pattern formation and criteria for pattern selection in homogeneous and heterogeneous models of a fixed catalytic bed for reactions with oscillatory kinetics (Sheintuch and Nekhamkina, 1999a,b). Stabilization of front solutions in distillation column have also recently attracted considerable interest (Kienle, 2000).

Front solutions in the infinitely long reaction–diffusion bistable system, $x_t - x_{zz} = f(x)$, have been extensively analyzed and several results have been derived for $f(x) = 0$ with multiple solutions (such as Mikhailov, 1990). We focus attention on the problem of front stabilization in a finite domain system with flow and subject to realistic boundary conditions.

Correspondence concerning this article should be addressed to M. Sheintuch.
Present address of V. Panfilov: Dept. of Mathematics, Ben-Gurion University, P.O. Box 653, Beer-Sheva 84105, Israel.

To admit multiple solutions we consider in the present work a reactor model that admits local bistability due to the interaction of nonlinear kinetics (due to exothermic-activated reaction) with heat loss due to cooling and with a mass generation source, either by a preceding reaction or by mass supply through the membrane wall (see Sheintuch and Nekhamkina, 1990a,b, or Barto and Sheintuch, 1994, for a detailed description). While this is not a common feature in current reactor design, problems of membrane reactor now attract considerable interest. After certain model-reduction procedures (see below), the system of interest can be approximately described by $x_t + Vx_z - x_{zz} = f(x)$ with bistable $f(x) = 0$. We can use three types of parameters for control: parameters that affect $f(x)$, the fluid velocity (essentially V), and parameters that affect the boundary conditions. We search for the technically simplest control: we study the global control and point-sensor control strategies; the latter is shown to be advantageous for stabilization of steep fronts.

The present problem also differs from fixed-bed models that may induce creeping-front solutions (Frank-Kamenetski, 1969; Luss, 1997). The latter can be approximately reduced to a similar form with $f(x)$ that does not change sign within the x-domain of interest. (The distinction between these two fronts is outlined in Benguria and Depassier, 1996.) The results derived from the present work will be used in a future publication to analyze creeping fronts in fixed beds.

The structure of this work is as follows. In the next section the mathematical model and its multiplicity features are studied in order to provide bistability conditions and to derive several stationary profiles of interest. The linear stability analysis of selected patterned states in an open-loop case is conducted in the third section. The Galerkin method, which is a conventional approach for lumping of the distributed parameter systems (DPSs), and problems of its application to control are briefly discussed, too. Various closed-loop case studies and their capabilities for the front stabilization are presented in the fourth section. A qualitative analysis based on reduction to a model that tracks the front position is conducted in the fifth section. The results are discussed in the concluding remarks.

Mathematical Model and Its Multiplicity Features

We investigate the following dimensionless system that describes the conversion (x), temperature (y), and catalyst activity (θ) in a cross-flow reactor

$$\frac{\partial x}{\partial t} + Pe_C\frac{\partial x}{\partial z} - \frac{\partial^2 x}{\partial z^2} = f_1(x,y,\theta) = Da\theta(1-x)E(y) - \alpha_C(x - x_w)$$

$$Le\frac{\partial y}{\partial t} + Pe_T\frac{\partial y}{\partial z} - \frac{\partial^2 y}{\partial z^2} = f_2(x,y,\theta) = BDa\theta(1-x)E(y) - \alpha_T(y - y_w)$$

$$\tau_\theta\frac{d\theta}{dt} = g(y,\theta) = -My - K_1\theta + K_0. \quad (1)$$

The terms on the lefthand side account for accumulation, convection, and conduction or diffusion (while surface activity θ is localized). Note that typically $Le \gg 1$ due to a large catalyst heat capacity, and Pe_T, $Pe_C \gg 1$. The terms on the righthand side of the mass and enthalpy balances account for a first-order exothermic and activated reaction, mass supply through the reactor wall (x_w is the wall concentration), and heat removal through it (y_w is the wall temperature). These two balances can admit multiple solutions for α_T, $\alpha_C \neq 0$. They are coupled with a slow deactivation–reactivator process ($\tau_\theta \gg 1$) that is written for simplicity in a linear form (see Barto and Sheintuch, 1994, for details). Danckwerts boundary conditions apply

$$\frac{\partial x}{\partial z}(0) = Pe_C x(0), \qquad \frac{\partial y}{\partial z}(0) = Pe_T y(0),$$

$$\frac{\partial x}{\partial z}(1) = 0 \qquad \frac{\partial y}{\partial z}(1) = 0, \quad (2)$$

where

$$E(y) = \exp\left(\frac{y}{1+y/\gamma}\right), \quad x = \frac{C_m - C}{C_{\text{in}}}, \quad y = \gamma\frac{T - T_{in}}{T_{in}},$$

$$z = \frac{\zeta}{L}, \; t = t'\frac{D_e}{L^2}, \; \gamma = \frac{E}{RT_{in}}, \; B = \gamma\frac{(-\Delta H)C_{in}D_e}{T_{in}k_e},$$

$$Da = e^{-\gamma}\frac{AL^2}{D_e}, \quad Pe_C = \frac{uL}{D_e}, \quad Pe_T = \frac{\rho_f c_{pf} uL}{k_e},$$

$$Le = \frac{\rho_s c_{ps} D_e}{k_e}, \quad \alpha_C = \frac{H_C PL^2}{D_e}, \quad \alpha_T = \frac{H_T PL^2}{k_e},$$

$$\tau_\theta = \frac{D_e}{k_{d\_}L^2}, \quad M = \frac{1}{\gamma}\frac{\mu T_{in}}{k_{d\_}}, \quad K_1 = \frac{k_{d\_} + k_{d+}}{k_{d\_}},$$

$$K_0 = \frac{k_{d+}}{k_{d\_}}. \quad (3)$$

Note that dependent variables are normalized in a standard way. The parameters are defined in a way that will allow us to consider various manipulated control parameters, and, in particular, to vary the flow velocity u only by varying the Pe numbers.

Stationary front solutions can be induced in a sufficiently long system (large Pe numbers) when $f_1(x,y,\theta) = f_2(x,y,\theta) = g(y,\theta) = 0$ (Eqs. 1) admits multiple steady states, that is, in a reactor with bistable source functions. Thus we look for the parameter set for which the source functions have three (or more) zeros. Such a problem can be reduced here to a single-variable representation

$$F(y) = \exp\left(\frac{y}{1-y/\gamma}\right)(P_1 y - 1)(y - P_2) - P_3(y - y_w) = 0$$

$$P_1 = M/K_0, \qquad P_2 = B\frac{\alpha_C}{\alpha_T}(1 - x_w) + y_w,$$

$$P_3 = \frac{\alpha_C}{Da}\frac{K_1}{K_0}. \quad (4)$$

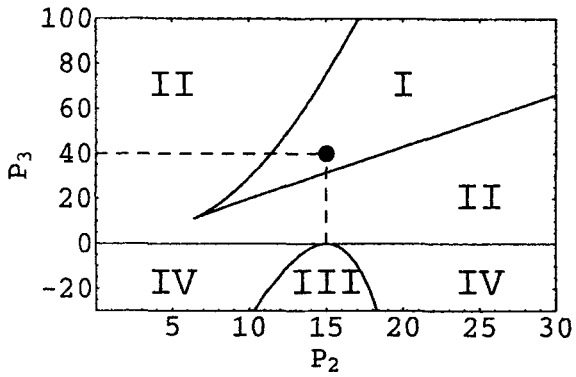

Figure 1. Bifurcation set of Eq. 4: the number of the source-function zeros.

Three physical (and one unphysical) solutions exist within region I: bold dot shows the point in parameter space for which steady states have been calculated (see Figures 3 and 4 for different sets of *Pe* numbers). II—region of 2 solutions. For mass loss case (α_C, $P_3 < 0$) the regions are: III—3 solutions, and IV—1 solution. The system parameters are $P_1 = M/K_0 = 1/15$, $y_w = 0$, $\gamma = 1/15$.

The bifurcation set is defined by the locus of the fold points, $F(y) = dF/dy = 0$. Figure 1 presents a cross section of the bifurcation set, with fixed parameters y_w, γ, P_1, that separates the (P_2, P_3) plane to regions differing in their number of $F(y) = 0$ solutions. Multiple solutions exist only in region I and a front then can be realized for certain *Pe* values. A typical bifurcation diagram is shown in Figure 2.

Steady-state solutions have been obtained by numerical simulations of the full model (Eqs. 1–2) using specific sets of *Le*, τ_θ values, for which the desired steady states are stable (typically, $\tau_\theta \ll Le$). Adjusting the *Pe* values we can arrest the moving front, and a stationary front profile can be observed. The calculation procedure employed an implicit finite difference scheme based on the method of fractional steps with up to 1,200 mesh points while verifying convergence with respect to cell size. The order of this scheme is $O(t^2, \Delta z)$ (Sheintuch and Nekhamkina, 1999a,b).

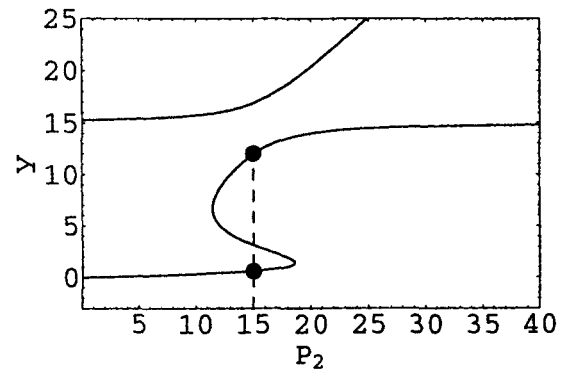

Figure 2. Bifurcation diagram of Eq. 4: dimensionless temperature *y* vs. P_2 parameter.

The central zone is a typical S-shaped curve with multiple solutions. Dots mark lower and upper zeros of the source functions at the parameter value ($P_2 = 15$) used for simulations. The highest branch is the unphysical one. Parameters as in Figure 1.

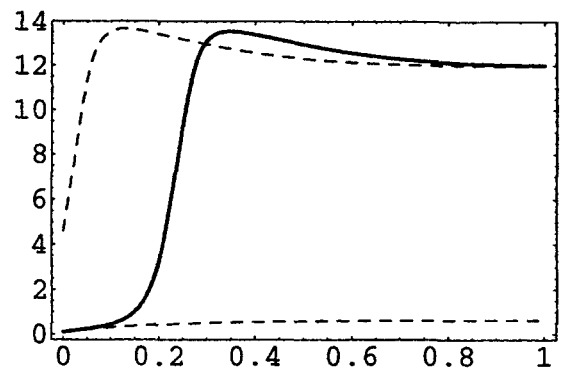

Figure 3. Temperature profiles for upper, lower, and front solutions.

Parameters: $Pe_T = Pe_C/2 = 26.125$; $B = 15$; $\gamma = 15$; $Da/Pe_C = 0.25$; $\alpha_C/Pe_C = 5$; $\alpha_T/Pe_T = 10$; $x_w = y_w = 0$; $M/Pe_C = 1/15$; $K_1/Pe_C = 2$; $K_2/Pe_C = 1$.

Figure 3 presents three inhomogeneous solutions computed for a certain set of parameters, and we refer to them as the lower, the upper, and the front solutions. All of them approach one of the homogeneous states on the right edge. If zero-flux boundary conditions would apply on both ends, then the lower and upper steady states would be truly homogeneous and correspond to the zeros of the source functions (marked by dots in Figure 2), while the front solution would be a steep curve approaching the lower state from the left and the upper state from the right. The inverse front connecting upper to lower states may be observable only in very rare cases, because of the inlet condition. Generally, the interaction between the fluid flow and front motion can produce an array of spatiotemporal patterns (Sheintuch and Shvartsman, 1996). Figure 4 presents the profiles of the front pattern for all three components of the model given by Eq. 1 calculated for another parameters set (with a larger *Pe*). An observed moving front is illustrated in Figure 5.

Open-Loop Linear Stability Analysis

We check the local stability of the nonlinear reactor model (Eqs. 1 and 2) using the Lyapunov linearization method

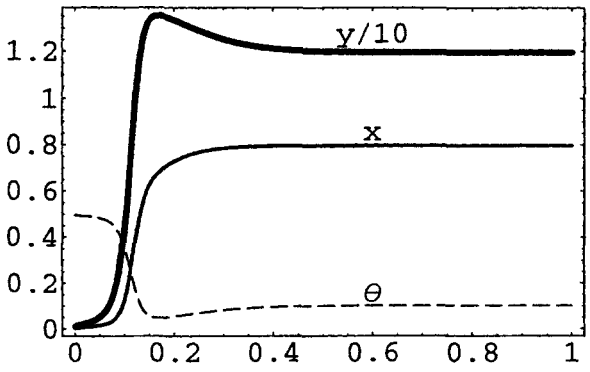

Figure 4. Profiles of all 3 components for the front solution.

The parameter set: $Pe_T = Pe_C/2 = 52.5$; $B = 15$; $\gamma = 15$; $Da/Pe_C = 0.5$; $\alpha_C/Pe_C = 10$; $\alpha_T/Pe_T = 20$; $x_w = y_w = 0$; $M/Pe_C = 1/15$; $K_1/Pe_C = 2$; $K_2/Pe_C = 1$.

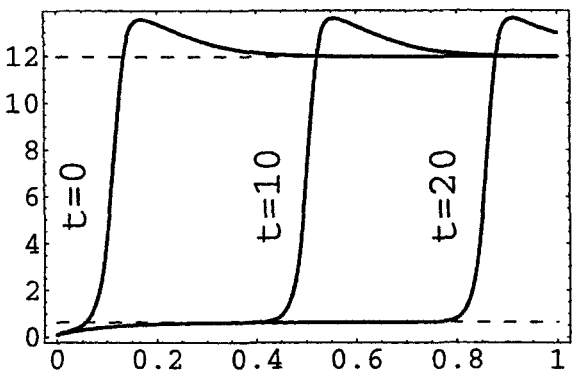

Figure 5. Moving (nonstationary) front: the temperature profiles

Dashed lines correspond to upper and lower zeros in Figure 2. Parameters as in Figure 4 with disturbed values $Pe_T = Pe_C/2 = 60$ and $Le = 100$, $\tau_\theta = 1$ (which corresponds to front stability region in Figure 8 below).

adapted for DPS. The Lyapunov linearization and the corresponding theorems make the relationship between stability of the linear system and the local stability of the original nonlinear system precise (such as Slotine and Li, 1991). In its first step the original nonlinear system is linearized around the desired steady state. Then a spectral decomposition of the Galerkin method is applied to the obtained linear distributed parameter system. This lumping technique using modal decomposition (such as Ray, 1981) is a common approach for DPS and it generally transforms the system of PDEs into an infinite dimensional system of ODE. At the last step the local stability properties of this (infinite dimensional) ODE system should be studied. This study is based, essentially, on reduced-order models. The question of whether it is possible to study and control an infinite dimensional system by a finite dimensional representation has received a principal positive answer for linear (and some classes of nonlinear) systems by Balas (1982, 1983, 1991): *consistent* Galerkin approximation of a sufficiently large order implies stabilization in a closed loop with the actual DPS. Moreover, an effect of the control spillover (degree of destabilization) caused by reduced-order representation can be estimated (Curtain, 1985; Sakawa, 1983).

Let us briefly discuss the technique of the analysis used. The original system (Eq. 1) can be rewritten in a short vector form

$$\boldsymbol{v}_t = \boldsymbol{f}(\boldsymbol{v}, \boldsymbol{u}), \tag{5}$$

where $\boldsymbol{v} = (x, y, \theta)^T$ is a vector of state variables, $\boldsymbol{u}$ is a general control input, and $\boldsymbol{f}$ is a vector-function incorporating terms of partial differentiation, source-functions, and control. Obviously, $\boldsymbol{f}$ satisfies the following conditions:

$$\boldsymbol{f}(\boldsymbol{v}_s, \boldsymbol{0}) = \boldsymbol{0}; \qquad \boldsymbol{f}(\boldsymbol{v}, \boldsymbol{0}) = \begin{pmatrix} -Pe_C x_z + x_{zz} + f_1 \\ (-Pe_T y_z + y_{zz} + f_2)/Le \\ g/\tau_\theta \end{pmatrix},$$

where $\boldsymbol{v}_s$ is a vector of steady-state solution.

The linearization of this nonautonomous (because of control) nonlinear system (Eq. 5) in terms of the perturbed state variables $\boldsymbol{v} = \boldsymbol{v}_s + \Delta\boldsymbol{v}$ yields

$$\Delta\boldsymbol{v}_t = \left(\frac{\partial \boldsymbol{f}}{\partial \boldsymbol{v}}\right)_{\boldsymbol{v}=\boldsymbol{v}_s, \boldsymbol{u}=0} \Delta\boldsymbol{v} + \left(\frac{\partial \boldsymbol{f}}{\partial \boldsymbol{u}}\right)_{\boldsymbol{v}=\boldsymbol{v}_s, \boldsymbol{u}=0} \boldsymbol{u}. \tag{6}$$

The boundary conditions should be linearized, too, and in our case keep their form (Eq. 2). The effect of the second control term will be considered in detail below. Now we consider the open-loop system, $\boldsymbol{u} = \boldsymbol{0}$.

Generally, the Jacobian matrix $\partial \boldsymbol{f}/\partial \boldsymbol{v}$ is spatially dependent and system (Eqs. 6 and 2) is infinite dimensional. As early as 1966 Wang noted that stability with respect to one norm in DPS does not imply stability with respect to another norm. Such a difficulty does not appear in a finite dimensional case, since all norms are equivalent.

To separate the variables by the Galerkin method we assume a solution of Eq. 6 for the i-state variable ($i = 1,2,3$; in our case) in the form

$$\Delta\boldsymbol{v}_i = \sum_j a_{ij}(t)\phi_{ij}(z), \tag{7}$$

where $j = 1,2,\ldots$ is the number of the spectral component in each expansion. The main requirement to the i-Galerkin basis is that it should satisfy the corresponding boundary conditions. Useful mathematical properties are achieved by the orthonormal condition with respect to some scalar product $\langle \phi_{ik}, \Phi_{il} \rangle$ (defined by a norm choice), where $\{\Phi_i\}$ is an adjoint basis.

The resulting lumped system in the open-loop case is

$$\langle \{\Phi_i\}, \Delta\boldsymbol{v}_{i_t} \rangle = \langle \{\Phi_i\}, \boldsymbol{f}_v \Delta\boldsymbol{v}_i \rangle, \quad i = 1,2,3; \Rightarrow \boldsymbol{a}_t = A\boldsymbol{a}, \tag{8}$$

where $\boldsymbol{a} = (a_{11}, a_{12}, \ldots, a_{21}, a_{22}, a_{31}, a_{32}, \ldots)^T$ is a time-dependent vector of spectral coefficients from Eq. 7, and A is a constant matrix that is a spectral image of the Jacobian matrix.

In the last and third step, the reduced-order technique is used to transform the ODE system (Eq. 8) to a finite dimensional one in order to find the eigenvalues of the matrix A and to check the stability properties of the original system (Eq. 5).

While this approach is quite common for DPSs, three choices are still to be made: What norm (scalar product) to be used? What Galerkin functions? What reduction-order approach should be used? A simple spatial integration along the system length is used as a norm, $\|\cdot\|^2 = \langle \cdot, \cdot \rangle = \int_0^1 (\cdot)^2 dz$. This L_2-norm is a conventional choice (see also Christofides and Daoutidus, 1998) based on physical (energy) properties; exponential stability with respect to this norm implies that the total energy of the system tends to zero as $t \to \infty$. [Wang (1996) gave an opposite example in which a wrong choice of the norm causes the system to be always unstable.]

The trigonometric orthonormal functions have been chosen for Galerkin expansion. The Danckwerts boundary con-

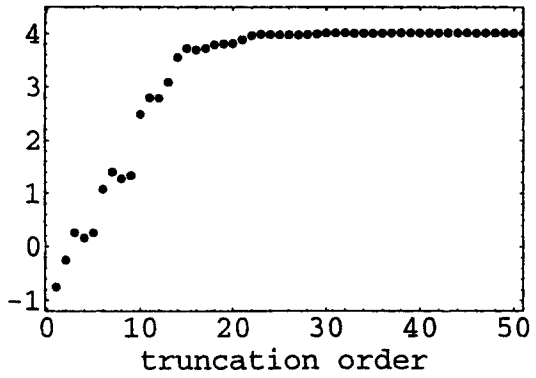

Figure 6. First eigenvalue (real part) vs. order of Galerkin truncation.

The data were calculated for the front solution in Figure 3, with $Le = 100$, $\tau_\theta = 100$.

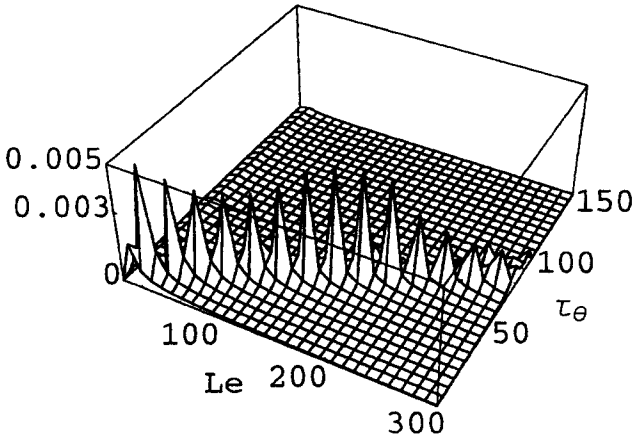

Figure 7. Accuracy of the eigenvalue calculation for various Le, τ_θ.

Absolute error in the first eigenvalue calculation for two successive Galerkin approximations (of orders 51 and 50) is shown.

ditions (Eq. 2) lead to the following functions

$$\phi_{ij} = \Phi_{ij} = \Lambda_{ij}\left[\cos(\lambda_{ij}z) + \frac{Pe_i}{\lambda_{ij}}\sin(\lambda_{ij}z)\right], \qquad i = C, T; \quad j = 1,2,\ldots,\infty, \quad (9)$$

where the parameters $\Lambda_{ij}, \lambda_{ij}$ can be calculated from the following formulas

$$\tan\lambda_{ij}, = Pe_i/\lambda_{ij}, \qquad i = C, T; \qquad j = 1, 2, \ldots, \infty$$

$$\Lambda_{ij} = \left\{ \int_0^1 \left[\cos(\lambda_{ij}z) + \frac{Pe_i}{\lambda_{ij}}\sin(\lambda_{ij}z)\right]^2 dz \right\}^{-1/2}. \quad (10)$$

Since the third component θ of the system (Eq. 1) is localized, the Galerkin basis for θ may be taken arbitrarily, for example, $\{\phi_T\}$, which is the same as for dimensionless temperature y.

The simplest reduction technique for consistent Galerkin approximations is a truncation of the Galerkin series, which can be used because of the dissipative nature of the parabolic model considered (Eq. 1). To estimate the desired approximation order we calculated the leading eigenvalues of matrix A for the front solution for increasing approximation order (Figure 6). Figure 7 shows that the accuracy for various sets of Le and τ_θ values is better than $5 \cdot 10^{-3}$ for a 51-order Galerkin approximation.

Thus in choosing the Galerkin functions and reducing the order, we follow the simplest approaches. Let us comment briefly on other possible approaches. Galerkin functions also can be determined by a solution of the eigenvalue problem of the convection–diffusion differential operator in Eqs. 1–2 (see, for example, Ray, 1981; Christofides and Daoutidus, 1996). The eigensystem obtained, then, is similar to Eq. 9, but has an additional factor $\exp(Pe_i z/2)$ [for the adjoint eigenfunction, it is $\exp(-Pe_i z)$], which creates serious numerical problems for the large Pe values used by us: a Galerkin approximation of 100 terms was insufficient to provide convergence. The Karhunen-Loeve expansion based on empirical eigenfunctions (see the recent review by Holmes et al., 1996) is a powerful tool because the required dimension of the reduced system is smaller, but is based on a large simulation database for each specific set of model parameters. On the contrary, in our case the Galerkin functions have been defined analytically by a single system parameter, Pe. One of the recent developments in model reduction methods is the nonlinear Galerkin method of approximate inertial manifolds that enables us to preserve qualitative dynamical features such as bifurcations, dissipation, and stability in the reduced model (Jones and Titi, 1994). Both methods have been used recently for controller design by Shvartsman and Kevrekidis (1998), but the reduced-order models were compared with those obtained by the conventional Galerkin method just described.

Linear stability analysis for each of the lower, the upper, and the front solutions was conducted for various time-scale constants (Le and τ_θ), since they do not influence the steady states. The 51-term approximation chosen earlier was used for the reduced-order model. The lower steady state is stable for all Le, τ_θ. The stable domains for both the stationary front and the upper stationary state are shown in Figure 8. Since for Le, $\tau_\theta \gg 1$ the mass balance is in pseudo-steady state, the stability is not affected by Le, and for large Le the τ_θ/Le stability boundary approaches an asymptotic value (Figure 8). Both the front and upper stationary patterns are stable for large Le values ($Le \to \infty$) and fixed τ_θ values, and instability appears above a certain threshold ($\tau_\theta/Le > 0.3$ in Figure 8). The transition from stable to unstable region (for $Le, \tau_\theta > 1$) for both upper and front states occurs via a Hopf bifurcation as two adjoint eigenvalues cross the imaginary axes.

To study the effect of the Pe numbers, the linear stability analysis has been conducted for an additional set of the system parameters by maintaining a relationship among the reactor parameters Da, α_C, α_T. Figure 8 indicates that an increase in Pe numbers reduces the stability domain for both front and upper solutions.

Control Strategies for the Front Stabilization

Before discussing the control strategies, we derive the general linearized form of the distributed control for Eq. 6 and

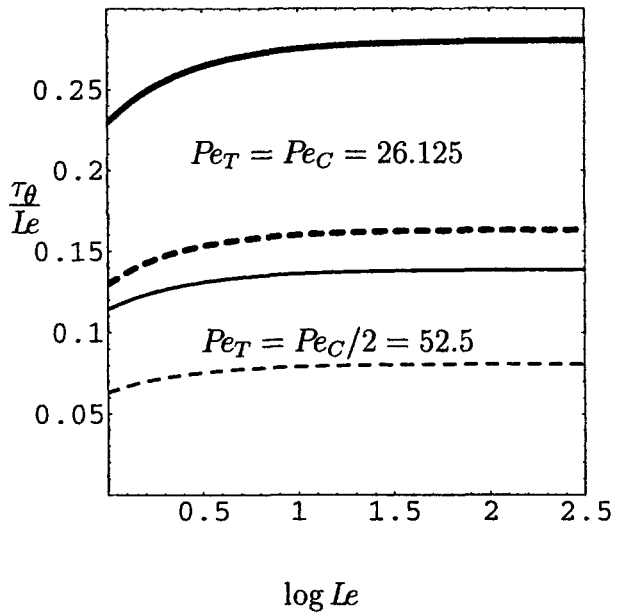

Figure 8. Open-loop stability of the front and upper solution in (τ_θ/Le, log Le) plane.

The state is stable below the line (that is a zero isoline of the real part of the maximal eigenvalue). Dashed or solid lines correspond to the upper or front solutions, respectively. Bold lines correspond to the parameter set, with smaller Pe values as in Figure 3, while regular lines correspond to the parameter set, with larger Pe values as in Figure 4.

demonstrate that its pole-placement capabilities are similar to the standard state feedback of the lumped system.

Let us consider a single distributed control action in Eq. 6 that can be written in a conventional decomposed form

$$u(z,t) = u(t)\psi(z), \tag{11}$$

where $\psi(z)$ is a space-dependent part of the distributed control that is an actuator influence function. Aside from useful mathematical properties, this decomposed form reflects the reality that, in most cases, the actuator influence device is constructively fixed and cannot be changed arbitrarily at any time. The time-dependent term $u(t)$ can be viewed as a sensor, and this term for feedback control can be expressed as the spatially weighted average of state variables, $v = (x, y, \theta)^T$ (this average can be nonlinear in the case of nonlinear control). The linearized form of the state feedback control and its spectral image for basic functions (Eq. 7) become

$$u(t) = \langle \Delta v_i, \Psi_i \rangle, \qquad i = 1,2,3: \quad \text{or} \quad u(t) = Ga, \tag{12}$$

where Ψ_i is a sensor weighted function of the i-state variable (such as $\Psi_i = 0$ if i-variable is not measured) and $G = (g_{11}, g_{12}, \ldots, g_{21}, g_{22}, \ldots, g_{31}, g_{32}, \ldots)$ is a constant row vector of spectral coefficients of these weighted functions. The vector G can be viewed as a gain matrix.

Substituting Eqs. 11 and 12 into Eq. 6 after integration yields

$$\langle \{\Phi_i\}, f_u \psi(z) \rangle u(t) = BGa, \qquad i = 1,2,3;$$

we obtain the closed-loop analog of the system given in Eq. 8

$$a_t = (A + BG)a, \tag{13}$$

where B is the spectral image of the general actuator function; for example, in the case of the single actuator Eq. 11, B is a vector. Thus the spectral image of a distributed parameter system is described in the standard form of the linear system with state feedback control. So, to provide the desired pole placement for appropriate matrix B, defined by actuator function $\psi(z)$, a gain matrix G determining sensor function $\Psi(z)$ can be chosen. Theoretically, there exists an infinite number of choices of control actions or sensors, but only a few may be practicable.

We plan to study the simplest control approaches by using the technically simplest actuators, as well as the simplest sensors. Thus, we restrict our discussion to the case $\psi(z) = 1$ and use time-dependent control only, $u(z,t) = u(t)$, with the technically simple sensors: *a global control*, in which a sensor responds to a spatially averaged property that can be measured by input and output fluxes, and *point-sensor control*, in which the deviation from a preset value is measured at a single point. The global control approach was tested for front stabilization in a reaction-diffusion system (Middya et al., 1994; Panfilov and Sheintuch, 1999). While it is easy to implement, it may be not sensitive enough for front stabilization. The simplest sensor of a chemical reactor is the temperature. Thus, we consider the two control approaches:

$$\text{Global control: } u(t) = k\langle y - y_s \rangle \tag{14}$$

$$\text{Point-sensor control: } u(t) = k[y(Z) - y_s(Z)] = k\langle y - y_s, \delta(z - Z) \rangle, \tag{15}$$

where k is a gain, Z is the location of the point sensor, and $\delta(z - Z)$ is a Dirac delta function. Note that in the case of the point-sensor control, two parameters (k and Z) can be varied.

Four closed-loop case studies, differing in the choice of the controlled parameter, are presented here. The first two involve manipulation of a parameter that directly affects the heat balance and the homogeneous steady state: we choose to vary either the heat-transfer coefficient (or practically the coolant flow rate), that is, α_T in Eq. 1 is replaced in a closed-loop system by the $\alpha_T[1 + u(t)]$ term, or the coolant temperature, that is, y_w is replaced by $[y_w - u(t)]$. The third approach is to vary the feed flow rate, that is, Pe_i is replaced by $Pe_i[1 + u(t)]$, $(i = C, T)$, which affects both the model equation and the boundary conditions, Eqs. 1 and 2. The last one is control via an inlet temperature, that is, the $Pe_i[-u(t)]$ term appears in the boundary conditions of Eq. 2. Note that since the choice of the Galerkin functions is defined solely by the boundary conditions, it would be desirable that any control in boundary conditions be replaced by some equivalent problem with unchanged boundary conditions, with $u(t)$ appearing on the righthand side of Eq. 1. Fortunately, any control in the boundary conditions can be replaced using the method of the Green function (see, for example, Ray, 1981), by the term on the righthand side with appropriate Dirac delta function as a factor [such as the $u(t)\delta(z)$ term appears in-

stead of $u(t)$ in the left boundary conditions].

To compactly describe each of the closed-loop case studies we present below the last term in the linearized system (Eq. 6). The control terms $f_u u$ for the closed-loop case studies have the following vector form (we keep the same order for vector components as in Eqs. 1):

$$c1.\ \alpha_T\text{-control:}\quad [0, \alpha_T(y_s - y_w)u(t), 0]^T$$

$$c2.\ y_w\text{-control:}\quad [0, \alpha_T u(t), 0]^T$$

$$c3.\ Pe\text{-control:}\quad \left[Pe_C\left(-x_{s_z} + x_s\delta(z)\right)u(t),\right.$$
$$\left. Pe_T\left(-y_{s_z} + y_s\delta(z)\right)u(t), 0\right]^T$$

$$c4.\ T_{in}\text{-control:}\quad (0, Pe_T\delta(z)u(t), 0)^T, \qquad (16)$$

where $u(t)$ takes one of the forms in Eqs. 14–15. Note that the spatially dependent factor in the linearized form just given can be viewed as a specified actuator function (see Eq. 11) that is achieved without technical changes in the system arrangement.

These control strategies have been applied to stabilization of the front shown in Figure 3. The first eigenvalue has been checked as a function of k, Le, τ_θ (and as a function of z for the point-sensor control) in the range $\tau_\theta \gg Le \gg 1$ and using a series truncated to 51 terms (as it was in an open-loop case).

The perfect *global control* (infinite gain, k) is ineffective and may only slightly increase the front stability domain for α_T-, y_w-control, as is evident by the stability boundaries plotted in Figure 9 and their comparison with the open-loop case. Moreover, control in inlet temperature (T_{in}-control) reduces the domain of front stability (Figure 9), and the perfect global control based on the fluid velocity makes the front unstable for any Le and τ_θ values: specific gain values can slightly reduce the magnitude of the eigenvalue, but cannot make it negative (Figure 10). We also checked a few combined global control methods (two control inputs), particularly control in Pe and α_T, each with its own gain value. Additionally, another sensor choice, based on α_C-global control in response to spatially average concentration, $u(t) = k\langle x - x_s\rangle$, was studied and found to be ineffective; similarly, combinations of the concentration and temperature global control, both introduced in Pe or, separately, in α_T, were studied and failed.

Point-sensor control of either the coolant flow rate (α_T) or the coolant temperature (y_w) can stabilize the front pattern within a certain domain of k and Z values, and the stabilization is attainable for any τ_θ, Le (Figures 11–12). To stabilize the front, the sensor should be placed sufficiently close to the front position, especially if $\tau_\theta \gg Le \gg 1$ (that is, away from the stability boundary). The results confirm the obvious observation that the front position is the most sensitive control signal. Point-sensor control in Pe (feed flow rate) or in T_{in} (inlet temperature) proved to be unable to stabilize the front when $\tau_\theta \gg Le \gg 1$.

Qualitative Analysis

The present problem is too complex for a detailed analysis. We try to present here a qualitative analysis based on a simplified model of control of a diffusion–convection–reaction system, by reducing the PDE model to a simple ODE that describes the front position, using an approximate expression for the front velocity. The model reduction is conducted in three steps.

First we capitalize on the high heat capacity ($Le \gg 1$) to assume that the concentration is in pseudo steady state. In that case, x can be expressed as a certain integral of y distribution. For the simple $Pe_T = Pe_C$ and $\alpha_T = \alpha_C$ case, the two balances can be added to find that at steady state x and y are linearly related ($y_s - Bx_s = y_w - Bx_w$). Under dynamic

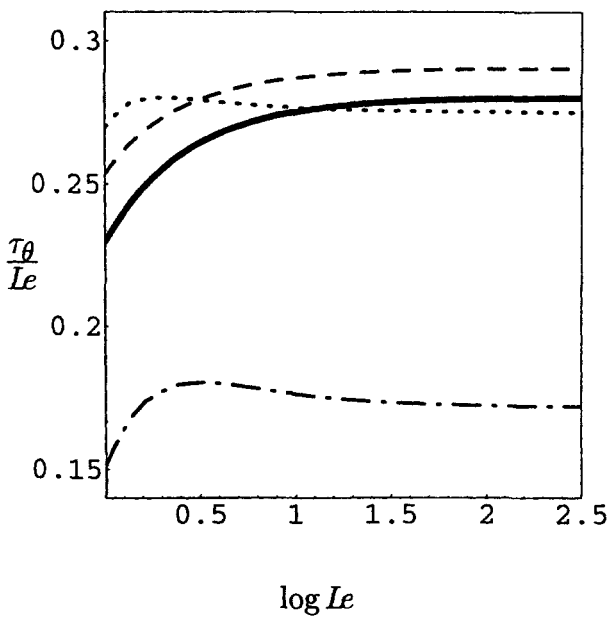

Figure 9. Closed-loop stability of the front under perfect (infinite gain) global control.

Bold solid line is the open-loop boundary, while dashed, dotted, and dot-dashed lines correspond to global control by manipulating α_T, y_w, and T_{in}, respectively. The parameters as in Figure 3. The perfect control via flow rate (Pe) makes the front unstable for large Le, τ_θ values (see Figure 10).

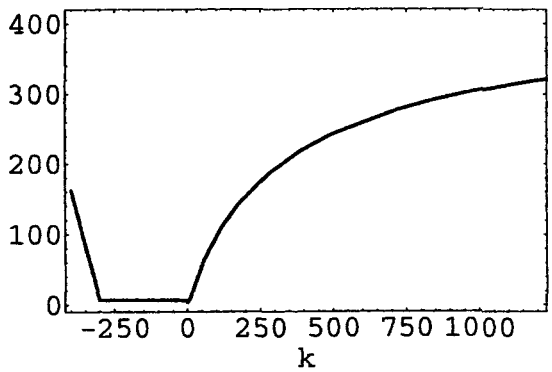

Figure 10. Global control in the feed flow rate (Pe numbers).

The real part of the first eigenvalue vs. gain value, k, is shown. Parameters as in Figure 3, with $Le = 100$, $\tau_\theta = 1{,}000$ corresponding to instability in the open-loop case (see Figure 8).

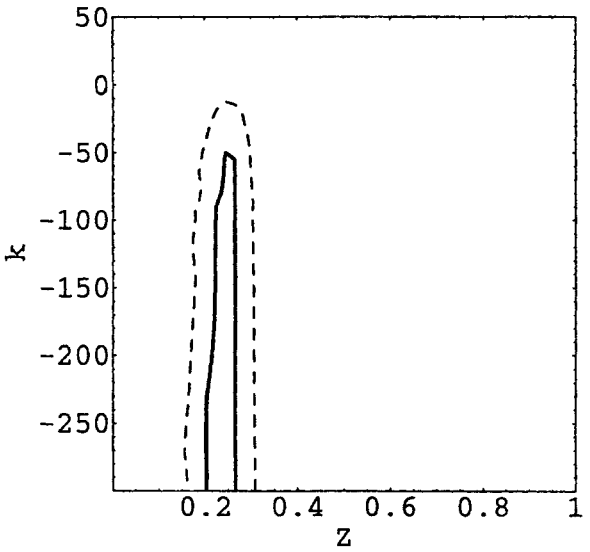

Figure 11. Point-sensor control in coolant flow rate, α_T.

The closed-loop stability domain (inside the line) is in the plane of sensor location, Z, vs. gain value, k. The parameters as in Figure 3, with $Le = 100$ and $\tau_\theta = 1{,}000$ or 40 shown by solid or dashed lines, respectively.

conditions this holds only approximately when the front motion is very slow. A similar analysis also can be conducted for the realistic case of infinite Pe_C, but will not be pursued here. Assume, therefore, that x and y are linearly related, $x = x(y)$, and the system is described by

$$Le\frac{\partial y}{\partial t} + Pe\frac{\partial y}{\partial z} - \frac{\partial^2 y}{\partial z^2} = f_2[x(y), y, \theta, p] \equiv F(y, \theta, p) \quad (17)$$

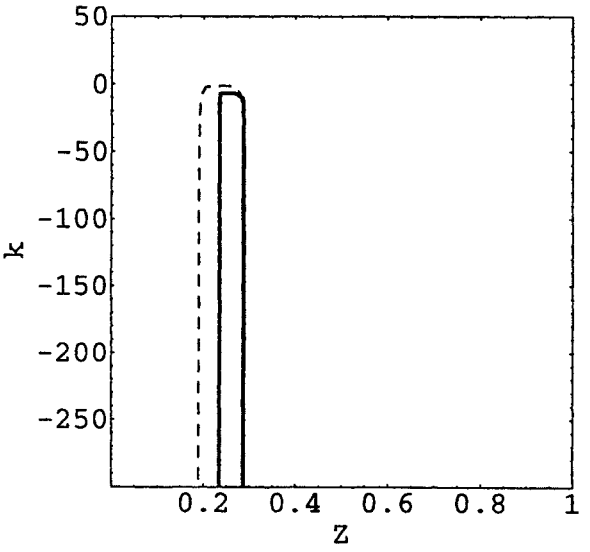

Figure 12. Point-sensor control in coolant temperature, y_w.

The stability domain in (Z, k) plane is larger than for control in Figure 11. The parameters as in Figure 3, with $Le = 100$ and $\tau_\theta = 1{,}000$ or 40 shown by solid or dashed lines, respectively.

$$\tau_\theta \frac{d\theta}{dt} = g(y, \theta), \quad (18)$$

subject to the boundary conditions specified in Eq. 2, where we have singled out the parameter (p) that will be used later for control purposes.

In the second step of model reduction we note that for $\tau_\theta \gg Le$ (or even when they are comparable) the activity profile is too slow to respond to the front motion and, since we are interested in small deviations from the set point, we can consider the activity profile to be frozen at its steady-state position, $\theta_s = \theta(y_s)$. The steady y_s and θ_s profiles are presented in Figure 4; the instability stems from the opposite inclination of the two: a perturbation of the front to the left will encounter higher activity, which will enhance its velocity, and so on. Thus, the model (Eqs. 17 and 18) can be reduced to the following form linearized with respect to p:

$$Le\frac{\partial y}{\partial t} + Pe\frac{\partial y}{\partial z} - \frac{\partial^2 y}{\partial z^2} = F[y, \theta_s(y_s), p^*] + F_p(p - p^*). \quad (19)$$

In the third step of the reduction we describe the front position approximately; that requires an expression for the front velocity of Eq. 19. While certain analytical results exist for the front velocity in an unbounded diffusion–reaction system of the form $y_t - y_{xx} = F(y)$, with an S-shaped source function and constant parameters, here we need to correct the front velocity for three terms: (1) the convective (or rather advective) flow, (2) the finite size and the boundary conditions, and (3) the spatially varying activity. The fluid-velocity effect on the front velocity is shown below. The edge effects on front velocity decay exponentially with the front distance from the edges, and for the sake of simplicity, we assume that the separation is sufficiently large to ignore it. (That also accounts for the inability to control the front position by manipulating the inlet conditions.) We will ignore the effect of the boundaries and focus on the effect of the parameter p. We will assume the activity affects the front velocity and its shape.

Assuming the existence of a shape-preserving front, its position (Z_f) is described by

$$\frac{dZ_f}{dt} = -c[\theta_s(Z_f), p]. \quad (20)$$

To find the velocity assume that the system is unbounded, and defining a new coordinate moving with the front $\xi = z - ct/Le$, we find its shape from

$$-\frac{\partial^2 y}{\partial \xi^2} - \frac{\partial y}{\partial \xi}(c - Pe) = F[y, \theta_s(y_s)^*, p], \quad (21)$$

where θ_s^* is the activity at the stationary front position. This equation is similar to that derived for a diffusion–reaction problem (that is, in the absence of convection), except that the front velocity is corrected by the fluid velocity, $-c = -c_{Pe=0} + Pe$. While analytical solutions exist only in a few cases (notably polynomial and piecewise linear F), we can

derive certain results from the theory of diffusion–reaction fronts. We can integrate Eq. 21 (after multiplying by $dy/d\xi$) to find

$$-(c-Pe)\int_{-\infty}^{\infty} y_\xi^2 d\xi - \frac{1}{2}y_\xi^2\Big|_{-\infty}^{\infty} = \int_{y_-}^{y_+} F(y,\theta_s^*,p)\,dy, \quad (22)$$

where $y_\mp$ are the solutions of $F(y,\theta_s^*,p)=0$. Note that the first integral on the left is positive, the second term vanishes for bounded system with no flux conditions, and the integral on the right determines the sign of $(c-Pe)$. Thus,

$$\frac{dZ_f}{dt} = -c = -c_{Pe=0} + Pe. \quad (23)$$

Now, the front is stationary for a certain $c^*(\theta^*,p^*)=Pe$, that is, under conditions that the kinetics counteracts the convective force. Now expand,

$$c_{Pe=0}(\theta_s,p) = c^*(\theta_s^*,p^*) + \frac{\partial c}{\partial\theta}(\theta_s-\theta^*) + \frac{\partial c}{\partial p}(p-p^*) \quad (24)$$

to find the dependence of the front position on activity and on the control variable. Since θ is assumed to be frozen for the short perturbation times considered, we can write

$$\theta_s(Z_f)-\theta^* = \left(\frac{\partial\theta}{\partial z}\right)_f (z-Z_s) = \left(\frac{\partial\theta}{\partial z}\right)_f (Z_f-Z_s), \quad (25)$$

where the subscript f denotes at the front position. Moreover, gradients in y and θ are related by

$$\left(\frac{\partial\theta}{\partial z}\right)_f = -\frac{g_y}{g_\theta}\left(\frac{\partial y}{\partial z}\right)_f, \quad (26)$$

where g_y, g_θ are evaluated at the setpoint (g is defined in Eq. 1).

We turn now to consider two control approaches based on point sensor and on global control. These are technically the simplest possible designs, since they are based on a single sensor that responds to either a local or the globally averaged temperature and a single space-independent actuator. In the first approach

$$p-p^* = k(y(Z)-y^*), \qquad y^* = y_s(Z_s), \quad (27)$$

where $y(Z_s)$ is the measured temperature at the sensor position, which was already chosen to be the setpoint position of the front, and y^* is the expected temperature at that point. We now show that this control essentially responds to changes in the front position. Assuming a perturbation that displaces the front position to Z_f without changing its shape, $y = y(Z_f)+(\partial y/\partial z)_f(z-Z_f)$, hence $y^* = y(Z_f)+(\partial y/\partial z)_f(Z_s-Z_f)$, and

$$p-p^* = k(\partial y/\partial z)_f(Z_f-Z_s). \quad (28)$$

Thus, from Eqs. 25, 26, and 28

$$\frac{dZ_f}{dt} = \left(\frac{\partial c}{\partial\theta}\frac{g_y}{g_\theta} - k\frac{\partial c}{\partial p}\right)\left(\frac{\partial y}{\partial z}\right)_f (Z_f-Z_s) \quad (29)$$

we conclude that a sufficiently large k will always stabilize the front.

In the global control approach the control responds to the changes in the average temperature front position by changing p, which affects the front velocity. Assuming perfect global control, we can satisfy the control condition without sufficiently affecting the velocity, and the control may fail then, as the numerical examples proved. If y_- and y_+ are the edge positions, and the front is narrow, then the average temperature at the set and perturbed positions follow

$$y_-(p^*)(Z_s)+y_+(p^*)(1-Z_s) = \langle y_s\rangle \quad (30)$$

$$y_-(p^*)(Z_f)+y_+(p)(1-Z_f) = \langle y_s\rangle. \quad (31)$$

Now, expanding $y_\mp(p) = y_\mp(p^*)+(\partial y/\partial p)_{F=0}(p-p^*)$, and rearranging, yields

$$p-p^* = (Z_f-Z_s)\frac{y_+(p^*)-y_-(p^*)}{\left(\frac{\partial y_-}{\partial p}\right)Z_f + \left(\frac{\partial y_+}{\partial p}\right)(1-Z_f)}. \quad (32)$$

The control effect is limited, therefore, by the term on the right, which may or may not be sufficient to stabilize the front, depending on the parameters and the destabilizing gradient of θ.

Convection affects the fluid velocity and the inventory conditions and its effect is more complex than that predicted by Eq. 23. These effects will be discussed in a future publication.

Conclusion

We have studied the problem of the stabilization of a front solution in a homogeneous reactor model for which several patterned states coexist. A simple model of a tubular catalytic reactor has been considered and is mathematically described by a system of the nonlinear parabolic equations with flow and is subject to Danckwerts boundary conditions. A spectral approach based on the Galerkin method was used to study the linear stability of the open-loop and controlled systems.

We consider four typical cases that are common for the mathematical model considered: control in a linear coeffi-

cient of the state variable, simple additive control, control in inlet flow, and direct boundary control (α_T-, y_w-, Pe-, and T_{in}-control, respectively). In each case, a specific spatially distributed control action has been achieved without artificial changes in the system construction, that is, only time-dependent control is considered. Two control-sensor strategies have been considered: global (spatially averaged sensing) and point-sensor control. The results show that y_w- or α_T-control with point-sensor control were effective for stabilization of the steep patterned states.

A qualitative analysis based on model reduction to a description of front position and a simplified model of front velocity showed how a parameter can be employed to stabilize the front using a point-sensor control based at the desired front position and why global control can fail to achieve that goal. The simplified approach did not account for the failure of control based on fluid velocity and that requires better approximation of the model.

Acknowledgments

One of the authors (V.P.) was supported by The Lady Davis Fellowship Trust and the Israel Science Foundation. The other author (M.S.) is a member of Minerva Center for Complex Systems. We are grateful to Prof. Hector Budman (Univ. of Waterloo) for very fruitful discussions on various aspects of the control methods, Dr. Boris Rubinshtein (Technion) for his contribution to development of the linear analysis tools, and Dr. Olga Nekhamkina (Technion) for the help in the numerical codes.

Notation

B = dimensionless exothermicity (defined in Eqs. 3)
C = front velocity
Da = Damkohler number (defined in Eqs. 3)
k = gain value of the feedback control
K_0, K_1, M = dimensionless deactivated parameters (defined in Eqs. 3)
Le = Lewis number (defined in Eqs. 3)
p = parameter singled out for control
Pe_C, Pe_T = mass and heat Peclet numbers (defined in Eqs. 3)
$u(z,t), u(t)$ = spatially distributed control and its time-dependent part
x, y, θ = dimensionless concentration, temperature, and activity
z = spatial coordinate
Z_F, Z_s = front position and its stationary value

Greek letters

α_C, α_T = dimensionless transport coefficient
γ = dimensionless activation energy (defined in Eqs. 3)
τ_θ = time scale of the deactivation process (defined in Eqs. 3)
ϕ_{ij}, Φ_{ij} = Galerkin functions and their adjoint functions of the i-state variable (defined in Eqs. 9–10)
ψ = actuator influence function of the spatially distributed control
Ψ_i = sensor control function for the i-state variable

Subscripts and superscripts

s = at the steady state
w = at the wall
$*$ = at the position of the stationary front

Literature Cited

Balas, M. J., "Toward a More Practical Control Theory for Distributed Parameter System," *Control and Dynamical Systems*, S. T. Leondez, ed., Vol. 18, Academic Press, New York, p. 361 (1982).
Balas, M. J., "The Galerkin Method and Feedback Control of a Linear Distributed Parameter Systems," *JMMA*, **91**, 527 (1983).
Balas, M. J., "Nonlinear Finite-Dimensional Control of a Class of Nonlinear Distributed Parameter Systems Using Residual Mode Filters: A Proof of Local Exponential Stability," *JMMA*, **162**, 63 (1991).
Barto, M., and M. Sheintuch, "Excitable Waves and Spatiotemporal Patterns in a Fixed-Bed Reactor," *AIChE J.*, **40**, 120 (1994).
Benguria, R. D., and M. C. Depassier, "Speed of Fronts of the Reaction-Diffusion Equation," *Phys. Rev. Lett.*, **6**, 1171 (1996).
Chen, G., *Control and Synchronization of Chaotic Systems (a bibliography)*, ECE Dept., Univ. of Houston (1996). (Available from ftp: uhoop.egr.uh.edu/pub/TeX/chaos.tex).
Christofides, P. D., and P. Daoutidus, "Nonlinear Control of Diffusion-Convection-Reaction Processes," *Comput. Chem. Eng.*, **20**, S1071 (1996).
Christofides, P. D., and P. Daoutidus, "Robust Control of Hyperbolic PDE Systems," *Chem. Eng. Sci.*, **53**, 85 (1998).
Curtain, R. F., "Pole Assignment for Distributed Systems by Finite-Dimensional Control," *Automatica*, **21**, 57 (1985).
Frank-Kamenetski, D. A., *Diffusion and Heat Transfer in Chemical Kinetics*, Plenum New York (1969).
Holmes, P., J. L. Lumley, and G. Berkooz, *Tubulence, Coherent Structures, Dynamical Systems and Symmetry*, Cambridge Univ. Press, New York (1996).
Jones, D. A., and E. S. Titi, "A Remark on Quasi-Stationary Approximate Inertial Manifolds for the Navier-Stokes Equations," *SIAM J. Math. Anal.*, **25**, 894 (1994).
Kienle, A., "Low-Order Dynamic Models for Ideal Multicomponent Distillation Processes Using Nonlinear Wave Propagation Theory," *Chem. Eng. Sci.*, **55**, 1817 (2000).
Luss, D., "Temperature Fronts and Patterns in Catalytic Systems," *Ind. Eng. Chem. Res.*, **36**, 2931 (1997).
Middya, U., D. Luss, and M. Sheintuch, "Spatiotemporal Motions Due to Global Interaction," *J. Chem. Phys.*, **100**, 3568 (1994).
Mikhailov, A. S., *Foundation of Synergetics I. Distributed Active Systems*, Springer-Verlag, Berlin (1990).
Ott, E., C. Grebogi, and J. A. Yorke, "Controlling Chaos," *Phys. Rev. Lett.*, **64**, 1196 (1990).
Panfilov, V., and M. Sheintuch, "Using Weighted Global Control for Stabilizating Patterned States," *Chaos*, **9**, 78 (1999).
Ray, W. H., *Advanced Process Control*, McGraw-Hill, New York (1981).
Sakawa, Y., "Feedback Stabilization of Linear Diffusion System," *SIAM J. Control Opt.*, **21**, 667 (1983).
Sheintuch, M., and S. Shvartsman, "Spatiotemporal Patterns in Catalytic Reactors," *AIChE J.*, **42**, 1041 (1996).
Sheintuch, M., and O. Nekhamkina, "Pattern Formation in Homogeneous Reactor Models," *AIChE J.*, **45**, 398 (1999a).
Sheintuch, M., and O. Nekhamkina, "Pattern Formation in Homogeneous and Heterogeneous Reactor Models," *Chem. Eng. Sci.*, **54**, 4535 (1999b).
Shvartsman, S., and Y. G. Kevrekidis, "Nonlinear Model Reduction for Control of Distributed Parameter Systems: A Computer Assisted Study," *AIChE J.*, **44**, 1579 (1998).
Slotine, J.-J., and W. Li, *Applied Nonlinear Control*, Prentice Hall, Englewood Cliffs, NJ (1991).
Wang, P. K. C., "Asymptotic Stability of Distributed Parameter System with Feedback Controls," *IEEE Trans. Automt. Contr.*, **AC-11**, 46 (1966).

Manuscript received Jan. 18, 2000, and revision received May 31, 2000.